Characterization of a novel, cytokine-inducible carboxypeptidase D isoform in haematopoietic tumour cells

Padraic G. P. O'MALLEY*, Shirley M. SANGSTER*, Salma A. ABDELMAGID*, Stephen L. BEARNE* and Catherine K. L. TOO*†[1]

*Department of Biochemistry and Molecular Biology, Sir Charles Tupper Medical Building, Dalhousie University, 5850 College Street, Halifax, Nova Scotia, Canada B3H 1X5, and †Department of Obstetrics and Gynecology, Dalhousie University, Halifax, Nova Scotia, Canada B3H 1X5

CPD-N is a cytokine-inducible CPD (carboxypeptidase-D) isoform identified in rat Nb2 T-lymphoma cells. The prototypic CPD (180 kDa) has three CP domains, whereas CPD-N (160 kDa) has an incomplete N-terminal domain I but intact domains II and III. CPD processes polypeptides in the TGN (*trans*-Golgi network) but the Nb2 CPD-N is nuclear. The present study identified a cryptic exon 1′, downstream of exon 1 of the rat CPD gene, as an alternative transcription start site that encodes the N-terminus of CPD-N. Western-blot analysis showed exclusive synthesis of the 160 kDa CPD-N in rat Nb2 and Nb2-Sp lymphoma cells. Several haematopoietic cell lines including human K562 myeloma, Jurkat T-lymphoma and murine CTLL-2 cytotoxic T-cells express a 160 kDa CPD-immunoreactive protein, whereas mEL4 T-lymphoma cells express the 180 kDa CPD. The CPD-immunoreactive protein in hK562 cells is also nuclear and cytokine-inducible. In contrast, MCF-7 breast cancer cells express only the 180 kDa CPD, which is mainly in the TGN. CPD/CPD-N assays using substrate dansyl-L-alanyl-L-arginine show approx. 98 % of CPD-N activity in the Nb2 nucleus, whereas MCF-7 CPD activity is enriched in the post-nuclear 10 000 ***g*** pellet. The K_m for CPD-N and CPD are 132 ± 30 and 63 ± 9 μM respectively. Specific activity/K_m ratios show that dansyl-L-alanyl-L-arginine is a better substrate for CPD-N than for CPD. CPD-N has an optimal pH of 5.6 (due to domain II), whereas CPD has activity peaks at pH 5.6 (domain II) and pH 6.5–7.0 (domain I). CPD and CPD-N are inhibited non-competitively by zinc chelator 1,10-phenanthroline and competitively by peptidomimetic inhibitor DL-2-mercaptomethyl-3-guanidinoethylthiopropanoic acid. The Nb2 CPD-N co-immunoprecipitated with phosphatase PP2A (protein phosphatase 2A) and α4 phosphoprotein. In summary, a cytokine-inducible CPD-N is selectively expressed in several haematopoietic tumour cells. Nuclear CPD-N is enzymatically active and interacts with known partners of CPD.

Key words: CPD-N (isoform of carboxypeptidase D), cytokine-inducible, haematopoietic tumour cell, kinetics, nuclear enzyme, prolactin.

INTRODUCTION

Rat metallocarboxypeptidase D [CPD (carboxypeptidase D)] is the only known CP (carboxypeptidase) with multiple CP domains. The digestive CPA and CPB, with an apparent molecular mass of 30 000–40 000 Da, and the peptide-processing CPE and CPM (50 000–60 000 Da) have single CP domains [1]. In contrast, CPD has a molecular mass of 180 000 Da and contains three CPE-like CP domains, a single transmembrane domain and a short C-terminal cytoplasmic tail. The three CP domains (I, II and III) of CPD are believed to be the result of tandem duplications of an ancestral gene and each domain is highly conserved across species [2]. Only domains I and II are enzymatically active [3,4]; however, the inactive domain III has retained some of the residues potentially involved in substrate binding, suggesting that it may play a role in the binding and presentation of protein or peptide substrates [5]. The CPD active site uses a glutamic residue and a tightly bound penta-co-ordinated Zn^{2+} cofactor to catalyse the cleavage of C-terminal basic amino acid residues [1]. CPD is enzymatically active over a broad pH range and is primarily membrane-bound in the TGN (*trans*-Golgi network) where it processes polypeptides or prohormones that transit the constitutive secretory pathway [4,6–8]. Significant amounts of CPD (~10 %) are also trafficked to and from the plasma membrane [9,10]. The cell-surface CPD has been shown to cleave extracellular substrates and generate arginine, resulting in enhanced nitric oxide production in macrophages [11].

Recently, we identified a full-length PRL (prolactin)-inducible cDNA encoding a novel, nuclear-targeted CPD isoform, designated CPD-N, in the rat PRL-dependent Nb2 and PRL-independent Nb2-Sp T-lymphoma cell lines [12]. The full-length rat CPD-N cDNA (3751 bp) has 99.9 % (3582/3583) nucleotide identity with the rat CPD cDNA (4377 bp) [12,13]. However, the 5′-end of the CPD-N cDNA has 148 unique bases that replace the first 750 bases of the CPD cDNA. Thus the predicted CPD-N protein has a lower molecular mass of 160 000 Da and its primary structure has an incomplete N-terminal CP domain I but intact domains II and III. In CPD-N, truncation of CP domain I includes loss of residues His^{139}, Glu^{142} and Arg^{208}, which are essential for Zn^{2+} co-ordination, and the triad $N^{217}RS^{219}$, which anchors the carboxylate group of the substrate. Antibodies raised against the conserved C-terminal end of CPD and CPD-N recognize a single immunoreactive band of 160 kDa (i.e. CPD-N) in Nb2 cells and, furthermore, show nuclear distribution of the Nb2 CPD-N [12]. Using isoform-specific primers for RT (reverse transcriptase)–PCR, the CPD-N transcript is detected exclusively in the rat Nb2 and Nb2-Sp lymphoma cells, whereas only the CPD transcript is detected in normal rat brain and lungs [12]. Northern-blot analysis

Abbreviations used: Co-IP, co-immunoprecipitation; CPA, carboxypeptidase A; FBS, fetal bovine serum; HS, horse serum; IL-2, interleukin-2; MGTA, DL-2-mercaptomethyl-3-guanidinoethylthiopropanoic acid; OP, 1,10-phenanthroline; PP2A, protein phosphatase 2A; PP2Ac, catalytic subunit of PP2A; PRL, prolactin; TFIIB, transcription factor IIB; TGN, *trans*-Golgi network.

The nucleotide sequence data reported will appear in GenBank®, EMBL, DDBJ and GSDB Nucleotide Sequence Databases under the accession numbers NM_012836 for rCPD and AF284830 for rCPD-N.

[1] To whom correspondence should be addressed (email ctoo@dal.ca).

shows rapid stimulation of CPD-N expression by PRL or IL-2 (interleukin-2) in the rat lymphoma cells. PRL also stimulates expression of the full-length CPD in human HepG2 hepatoma and MCF-7 breast cancer cell lines. These studies indicate that hormones and cytokines (e.g. PRL and IL-2) can regulate the expression of CPD and CPD-N and, furthermore, suggest that PRL plays a role in regulating CPD/CPD-N processing of polypeptides in the TGN or other protein substrates in the cell nucleus [12].

The present study shows that the CPD-N transcript probably arises from an alternative promoter start site in the rat CPD gene, giving rise to the predicted 160 kDa CPD-N protein in rat Nb2 and Nb2-Sp lymphoma cells. Antibodies raised against the common C-terminal end of CPD/CPD-N also detected a nuclear 160 kDa protein in several mouse and human haematopoietic tumour cells. We also show that nuclear CPD-N in Nb2 cells is enzymatically active and interacts with protein partner(s) of the prototypic CPD.

MATERIALS AND METHODS

Antibodies

Anti-CPD/CPD-N polyclonal antibodies were raised against a common 15 amino acid region in the C-terminal tail of CPD or CPD-N, and the IgG was purified as described previously [12]. The anti-α4 phosphoprotein antibodies used have also been described previously [14]. Polyclonal antibodies directed to TFIIB (transcription factor IIB), glucokinase and horseradish peroxidase-linked secondary goat anti-mouse IgG were purchased from Santa Cruz Biotechnology (Santa Cruz, CA, U.S.A.). Monoclonal anti-PP2A (where PP2A stands for protein phosphatase 2A; catalytic subunit) was purchased from Transduction Laboratories (Mississauga, ON, Canada). Secondary donkey anti-rabbit IgG was obtained from Amersham Biosciences (Baie d'Urfé, QC, Canada).

Cell culture

Suspension cultures of the PRL-dependent rat Nb2-11C (Nb2) lymphoma cell line were routinely maintained in Fischer's medium (Sigma, Oakville, ON, Canada) for leukaemic cells containing 10 % (v/v) FBS (fetal bovine serum; as a source of lactogens) and 10 % lactogen-free HS (horse serum) as described previously [15]. For growth arrest, Nb2 cells were cultured in the medium containing 10 % HS alone for 18–24 h. Nb2 cell growth is also stimulated by IL-2; thus, the HS was also IL-2-free. The PRL-independent rat Nb2-Sp cell line was maintained in 10 % HS–Fischer's medium. Human MCF-7 breast cancer cell line, Jurkat T-leukaemic cell line and K562 myeloma cell line were all cultured in Dulbecco's modified Eagle's medium containing 10 % FBS. Mouse EL4 T-cell lymphoma and CTLL-2 cytotoxic T-cells were maintained in RPMI 1640 with 10 % FBS; CTLL-2 cells are IL-2-dependent and also received 20 ng/ml IL-2. MCF-7 and K562 cells express receptors for PRL and IL-2 respectively. Quiescent cells were obtained by culturing cells in 10 % HS (PRL- and IL-2-free) for 18–24 h before hormone treatment.

Subcellular fractionation and Western-blot analysis

For whole cell lysates, cells [(10–20) $\times$ 10^6] were harvested at 200 ***g*** for 5 min and lysed in cold RIPA buffer (50 mM Tris/HCl buffer, pH 7.4, 150 mM NaCl, 1 mM EGTA, 50 mM sodium pyrophosphate, 0.25 % sodium deoxycholate, 0.1 % Nonidet P40 and 1 mM NaF) containing 3 μg/ml each of aprotinin, leupeptin, pepstatin and 2 mM PMSF for 30 min on ice. The cells were further disrupted by gentle passage through a 23-gauge needle. Protein concentrations were determined using a Bio-Rad DC™ Protein Assay kit (Bio-Rad Laboratories, Mississauga, ON, Canada) and all samples were stored at -20 °C until further analysis.

For subcellular fractionation, Nb2 and MCF-7 cells [(10–20) $\times$ 10^6] were harvested at 200 ***g*** for 5 min, lysed in RIPA buffer (without detergent) for 30 min on ice and further disrupted by gentle passage through a 21-gauge needle. Whole cell homogenates, nuclear (700 ***g*** pellet, 5 min), organelle (10 000 ***g*** pellet, 25 min), microsomal (100 000 ***g*** pellet, 60 min) and cytosolic (100 000 ***g*** supernatant, 60 min) fractions were obtained. Protein concentrations were determined, Triton X-100 was added to a final concentration of 0.1 % (v/v) and samples were stored at -20 °C. SDS/PAGE was performed using 10–30 μg of protein/lane, representing approx. 15 % of the total protein in each fraction.

Western blotting was performed with the following primary antibodies: anti-CPD/CPD-N (15 μg/ml IgG), anti-TFIIB (1 μg/ml) and anti-glucokinase (2 μg/ml). Horseradish peroxidase-conjugated secondary antibodies, donkey anti-rabbit IgG and goat anti-mouse IgG were used at 1:5000 and 1:1500 dilution respectively. Immunoreactive signals were detected with Super Signal ULTRA kit (Pierce, Rockford, IL, U.S.A.).

Co-IP (co-immunoprecipitation)

Cells were harvested with RIPA buffer and precleared with Protein A/G–agarose (Santa Cruz Biotechnology) at 4 °C for 1 h. Samples were then centrifuged at 800 ***g*** for 5 min at 4 °C and 1.0 μg of primary antibody was added to the supernatant. Protein A/G–agarose was added 1 h later and the samples were rocked overnight at 4 °C. The pellet was again collected by centrifugation at 800 ***g*** for 5 min and washed twice with 1 ml of cold PBS. SDS/PAGE sample buffer was added for Western blotting.

Immunofluorescent confocal microscopy

Suspension cultures of K562 cells were cytospun on to silinized microscope slides, dried in cold acetone, fixed in 1 % paraformaldehyde and permeabilized in 0.1 % Triton X-100 as described previously [12]. The permeabilized cells were incubated with the primary antibody (1:10 of 4 mg/ml anti-CPD/CPD-N IgG in 0.1 % BSA/PBS) for 1 h at room temperature (18 °C) and washed three times in PBS before incubation with secondary antibody (1:50 of AlexaFluor 488 goat anti-rabbit IgG conjugate) for 1 h in the dark. After three PBS washes, the cells were incubated with propidium iodide (50 ng/ml in 0.1 % BSA) for 10 min. After a final series of PBS washes, a drop of Citifluor–glycerol/PBS AF1 solution (Marivac Halifax, Halifax, NS, Canada) was added and the slides were mounted with coverslips. Immunofluorescence was detected by confocal microscopy at $\times$ 100 magnification. MCF-7 cells were cultured on coverslips and were similarly processed as the K562 cells. At the final stage, a drop of Citifluor was added to each coverslip that was then mounted on a microscope slide.

Preparation of the dansyl-L-alanyl-L-arginine substrate

The CPD substrate dansyl-L-alanyl-L-arginine was synthesized by reacting dansyl chloride with the dipeptide, alanine–arginine as described previously [16–18]. Substrate purity was confirmed using TLC on 1 mm silica with chloroform/methanol (1:1) and a single fluorescent spot ($R_F = 0.7$) was detected by a Varian Cary Eclipse fluorescence spectrophotometer, indicating that the material was $>$ 99 % pure.

CPD/CPD-N enzyme assay

Nb2 and MCF-7 cells [(10–20) $\times$ 10^6] were homogenized with a 21-gauge needle in 0.1 M sodium acetate buffer (pH 5.6). Total

cell lysates or subcellular fractions were prepared (see above) and then Triton X-100 was added to each fraction to give a final concentration of 0.1 % (v/v). Samples were stored at −20 °C until further analysis. CPD activity was determined using an endpoint fluorescence assay as described previously [7,18]. Briefly, the ice-cold enzyme sample (60–80 ng of protein/μl in a total volume of 50 μl) was preincubated with 150 μl of 0.1 M sodium acetate buffer (pH 5.6) at 37 °C for 5 min. The assay was initiated by the addition of pre-equilibrated (37 °C) dansyl-L-alanyl-L-arginine substrate (in 50 μl of 0.1 M sodium acetate buffer, pH 5.6). After a 37 °C incubation (6 min for CPD-N and 10 min for CPD), the reaction was terminated by the addition of 150 μl of 1 M citric acid and the sample was placed on ice. The product dansyl-L-alanine was separated from the more hydrophilic substrate, dansyl-L-alanyl-L-arginine, by extraction with chloroform. Fluorescence in the chloroform layer was measured relative to a chloroform blank at 340 nm excitation wavelength and 495 nm emission. Dansyl-L-alanine (Tokyo Chemical Industry America, Portland, OR, U.S.A.) was used at various concentrations to construct a standard curve for each assay to correct for the perturbations in extraction efficiency. The inhibitors used were MGTA (DL-2-mercaptomethyl-3-guanidinoethylthiopropanoic acid; Calbiochem, La Jolla, CA, U.S.A.) and OP (1,10-phenanthroline; Sigma). For pH profile experiments, 0.1 M NaOAc was used for pH 3.5–5.6 and 0.1 M sodium phosphate (NaH_2PO_4/Na_2HPO_4) was used for pH 6.0–7.5. CP activity was determined as the difference in activity in the presence or absence of 10 μM MGTA. Specific activity SA was calculated as V_{max} (μmol/min = unit) per mg of protein (i.e. SA = unit/mg of protein).

RESULTS

Analysis of rat CPD-N and CPD cDNAs

The rat genome database [NCBI (National Center for Biotechnology Information)] was used to analyse the rat CPD and CPD-N cDNAs. Our analysis showed that 750 bases specific to the 5′-end of CPD cDNA were lost in the CPD-N cDNA and 148 additional bases unique to the 5′-end of the CPD-N cDNA were added [12]. These alterations are probably caused by an alternative start site resulting in transcription initiation at exon 1′, downstream of exon 1 (Figure 1). This would also result in the loss of any N-terminal signal peptide. In CPD, the signal peptide is responsible for both the trafficking of CPD into the lumen of the endoplasmic reticulum and for the insertion of CPD into the membrane of the TGN [1,5]. The absence of a signal peptide from CPD-N may dictate its alternative distribution in the cell nucleus.

Expression of CPD/CPD-N in haematopoietic cells

The full-length rat CPD cDNA has 92 and 83 % nucleotide identity with the mouse and human CPD cDNAs respectively. CPD-N-specific primers were initially designed for the unique 5′-end of the Nb2 CPD-N cDNA to yield a 264 bp PCR product [12]. BLAST analysis showed that the forward and reverse primers annealed to regions within the putative exon 1′ and exon 2 of the rat CPD genomic sequence respectively (Figure 2A). Although BLAST and Amplify 1.0 analyses revealed potential annealing sites in similar regions in the mouse and human CPD genomic sequences, the nucleotide identity was not fully conserved (Figure 2B). Furthermore, no open reading frame that would produce a 160 kDa CPD-N-like protein was identified in the corresponding regions of the mouse and human CPD genes.

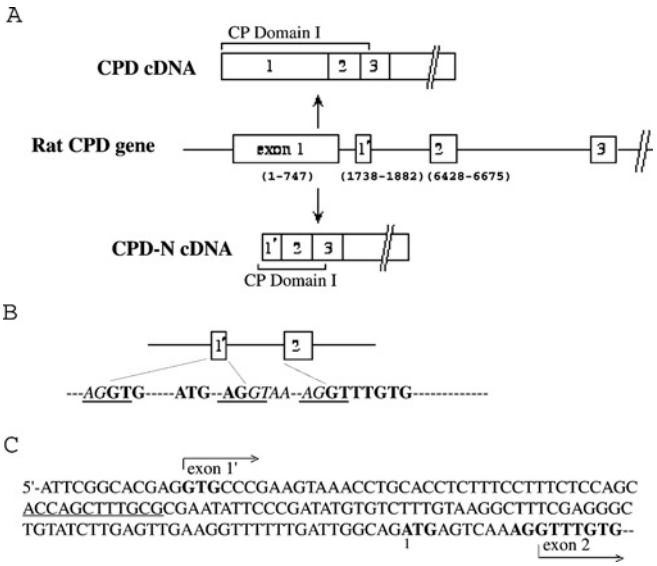

Figure 1 Schematic representation of the rat CPD gene

(**A**) The CPD cDNA is transcribed from exon 1 (nt 1–747), whereas the nuclear isoform CPD-N arises from a downstream exon 1′ (nt 1738–1882). Exon 1 encodes the N-terminus of CPD domain I. Exon 1′ encodes four unique amino acids in the N-terminus of the truncated CPD-N domain I. Nucleotide numbers are shown in parentheses. (**B**) The intron–exon boundaries of exon 1′ are underlined, with intron bases in italics and exons in boldface. The ends of introns show the appropriate splice donor–acceptor consensus sequences GT-AG. (**C**) The 5′-end of the cloned CPD-N cDNA. The bases in boldface including the ATG initiation codon are similar to those shown in (**B**). The forward primer used in Figure 2 is underlined. GenBank® accession numbers are NM_012836 for rCPD and AF284830 for rCPD-N.

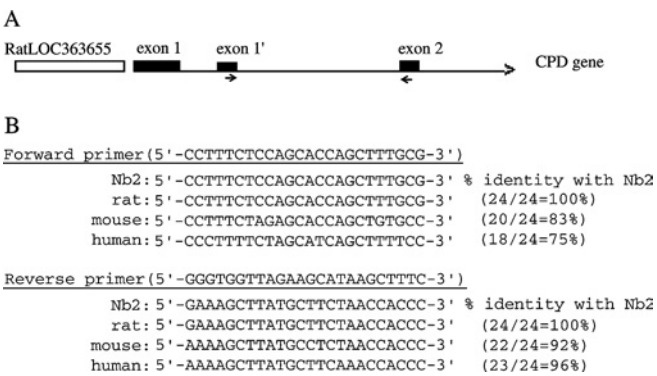

Figure 2 BLAST analysis of CPD-N primers against rat, human and mouse CPD genes

(**A**) Arrowheads show the annealing sites of the Nb2 CPD-N-specific primers which yielded the 264 bp PCR product previously reported [12]. (**B**) BLAST analyses showed 100 % base identity of the forward and reverse primers with the annealing sites in the rat CPD gene, but less than 100 % identity with corresponding regions in the mouse and human CPD genes.

Therefore Western-blot analysis was performed using CPD/CPD-N-specific antibodies to determine if the 160 kDa and/or 180 kDa CPD-immunoreactive protein was expressed in murine and human lymphoid tumour cells lines. Human MCF-7 breast cancer cells were used for comparison since we have shown by RT–PCR, using hCPD-specific primers, that PRL stimulated CPD expression (but not CPD-N) in these cells [12]. Figure 3 shows exclusive synthesis of the 180 kDa CPD in MCF-7 cells and the 160 kDa CPD-N in Nb2 and Nb2-Sp cells (Figures 3A and 3B). A 160 kDa immunoreactive band was detected in human K562

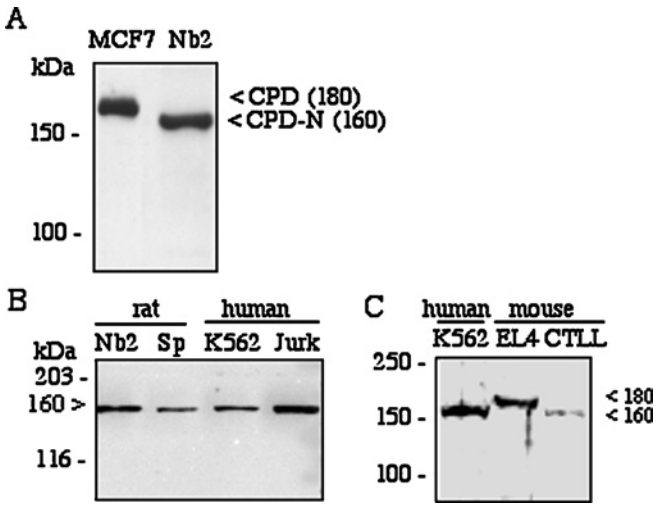

Figure 3 CPD/CPD-N protein expression

Whole cell homogenates of actively growing cells were used for Western-blot analysis. (**A**) MCF-7 cells synthesize the 180 kDa CPD, whereas Nb2 and Nb2-Sp cells (Sp) synthesize the 160 kDa CPD-N. (**B**) A 160 kDa immunoreactive band is present in human K562 and Jurkat (Jurk) cells. (**C**) Murine EL4 and CTLL-2 (+ IL-2) cells synthesized 180 and 160 kDa proteins respectively. Results shown are representative of two to three independent experiments.

myeloid or Jurkat T-leukaemic cells (Figures 3B and 3C). A single immunoreactive band of 180 or 160 kDa was detected in murine EL4 T-lymphoma and CTLL-2 cytotoxic T-cells respectively (Figure 3C). It is possible that the 160 kDa immunoreactive band is a spliced product from an unidentified start site in the human or mouse CPD gene. However, we cannot rule out the possibility that this smaller protein detected in the human and mouse samples was processed post-translationally from the mature 180 kDa CPD.

Localization of CPD-N

Previously, we demonstrated nuclear distribution of 160 kDa CPD-N in Nb2 cells using immunofluorescence confocal microscopy [12]. Here we examined the subcellular distribution of the 160 kDa protein in K562 myeloma cells and compared it with the distribution of the 180 kDa CPD in MCF-7 breast cancer cells. Figure 4(A) reveals that CPD has a perinuclear distribution in MCF-7 cells, consistent with its reported predominance in the TGN [9,19]. However, some punctate nuclear staining was also observed. In contrast, immunofluorescence of the 160 kDa protein was detected in both the nucleus of quiescent K562 cells and in the cytosol after treatment with IL-2 for 24 h (Figure 4B), further supporting the presence of a nuclear CPD-N immunoreactive protein in other lymphoid tumour cells. The appearance of immunofluorescence in the cytosol is consistent with IL-2 stimulation of CPD-N protein synthesis.

Co-IP of CPD-N protein partners

The serine/threonine phosphatase PP2A is known to bind to the cytoplasmic tail of CPD as a trimeric complex consisting of A (regulatory), B (variable) and C (catalytic) subunits [20]. Co-IP analysis showed that CPD-N in Nb2 cells interacted with PP2Ac (catalytic subunit of PP2A) (Figure 5A), demonstrating that the protein–protein interactions characteristic of the C-terminus of CPD are preserved in the CPD-N isoform. The different intensities of the immunoreactive bands corresponding to CPD-N and PP2Ac (Figure 5A) suggested that most of the CPD-N molecules were bound to PP2Ac but only a fraction of the PP2Ac molecules interacted with CPD-N.

PP2Ac is a known partner of α4 phosphoprotein [14,21], a protein component of the mTOR (mammalian target of rapamycin) pathway that regulates protein translation [22]. Both PP2Ac and α4 phosphoprotein are found predominantly in the Nb2 cell nucleus [14]. Thus it was not surprising to find an interaction of CPD-N with the α4 phosphoprotein in the Nb2 cells (Figure 5B, left panel). However, the reverse Co-IP using anti-α4 antibodies precipitated PP2Ac only but not CPD-N (Figure 5B, right panel), suggesting that α4 might be sequestered in the CPD-N–α4–PP2Ac complex and not available to the anti-α4 antibodies.

Kinetic properties of CPD-N and CPD

To measure CP enzymatic activities, Nb2 and MCF-7 cells were used as the sources for CPD-N and CPD respectively. Subcellular fractionation showed CPD-like activity in Nb2 cells that was almost entirely (~98 %) nuclear (Figure 6A). In contrast, CPD activity in MCF-7 cells was enriched in the post-nuclear fraction (10000 ***g***; Figure 6A, PNO) but some activity was also detected in the nuclear, microsomal and cytosolic fractions (Figure 6A).

Western-blot analysis detected abundant CPD-N (160 kDa) in the Nb2 cell nucleus (Figure 6B), which is in agreement with the cellular distribution indicated by enzymatic activity (Figure 6A). The distribution of CPD activity in MCF-7 cells is also consistent with the nuclear and perinuclear (i.e. TGN) staining for CPD (Figure 4A) and the detection of the CPD protein in the TGN and membrane fractions reported by others [9,19,23]. The detection of cytosolic glucokinase and a nuclear TFIIB confirmed fraction integrity (Figure 6B).

The kinetic properties of CPD-N and CPD were further examined using the Nb2 nuclear and MCF-7 PNO fractions respectively. Michaelis–Menten and Lineweaver–Burk plots for CPD-N (Figure 7) and CPD (results not shown) were used to determine their apparent K_m and V_{max} values (Table 1). The apparent K_m values were 132 ± 30 and 63 ± 9 μM for CPD-N and CPD respectively, suggesting that CPD binds dansyl-L-alanyl-L-arginine with twice the affinity exhibited by CPD-N.

To characterize further the two isoforms, inhibition studies were conducted using the potent peptidomimetic inhibitor MGTA and the Zn^{2+}-chelator OP. MGTA is a strong competitive inhibitor of CPD at nM concentrations, whereas OP is a less potent non-competitive inhibitor and is typically used at μM concentrations [4]. Lineweaver–Burk plots for the inhibition of CPD-N in the presence of MGTA (Figure 8A) or OP (Figure 9A) indicated competitive inhibition by MGTA and non-competitive inhibition by OP. Furthermore, plots of K_m/V_{max} versus inhibitor concentrations were used to determine the inhibition constants (K_i) of MGTA (Figure 8B) and OP (Figure 9B). In addition, MGTA and OP inhibition of CPD was determined similarly (results not shown). Table 2 shows that the K_i values for the inhibition of CPD-N by MGTA and OP are approx. 5-fold less than those for CPD. Thus both CPD and CPD-N exhibited competitive inhibition with MGTA and non-competitive inhibition with OP.

Optimal pH of CPD and CPD-N

CPD is believed to process polypeptides or prohormones as they transit the TGN–endosomal pathway and is active over a broad pH range (pH 5–7), presumably permitting the enzyme to function at the varying pH values encountered along the secretory pathway [1]. CP domain I is optimally active at a neutral pH, whereas domain II has an optimum pH of 5.6 [4]. Since CPD-N lacks a functional domain I, it was expected to be active only in the lower

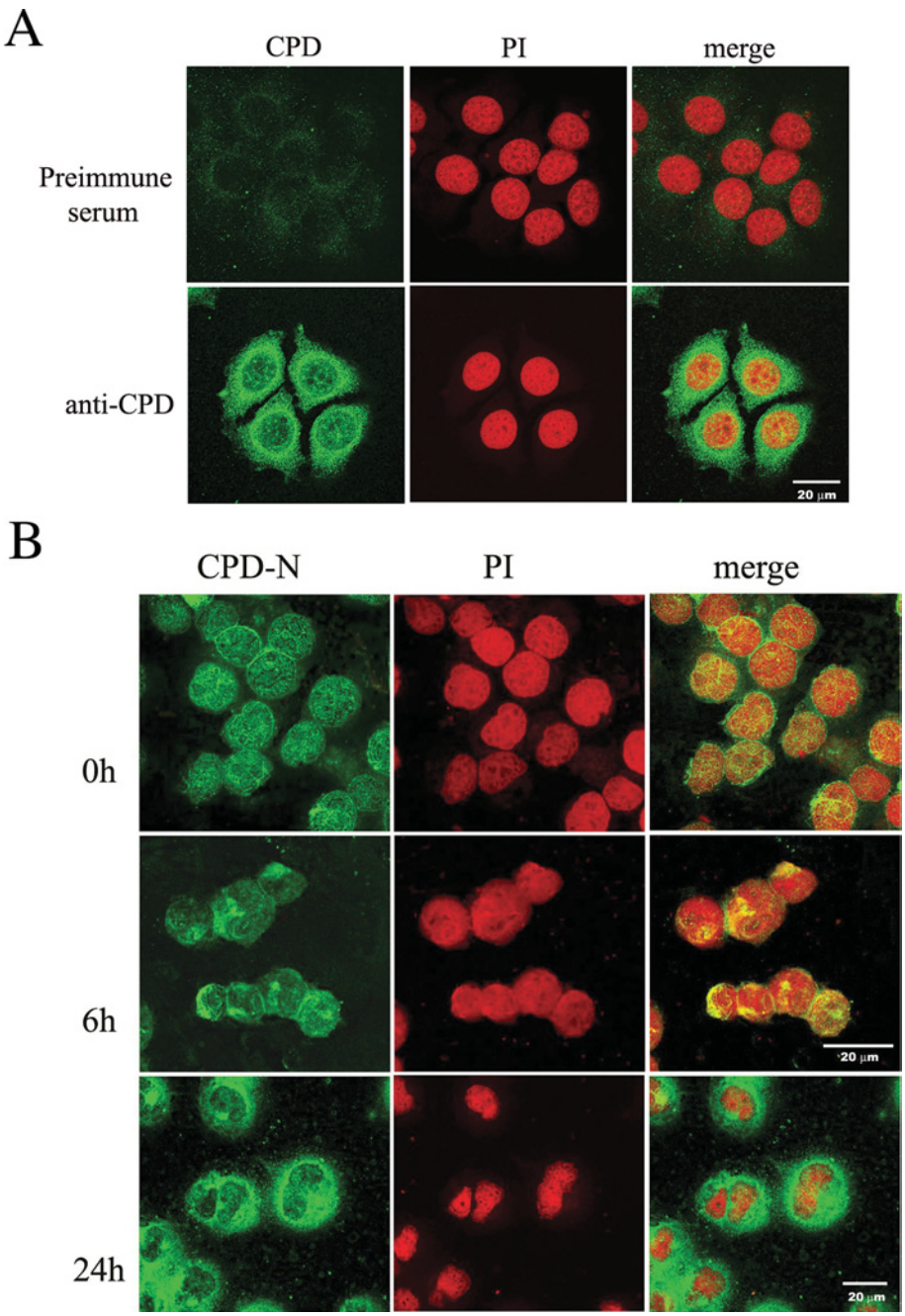

Figure 4 Confocal microscopy showing CPD-N localization

(**A**) Exponential-phase growing MCF-7 cells and (**B**) K562 cells, either quiescent (0 h) or treated with IL-2 for 6 and 24 h, were prepared as described in the Materials and methods section. Cells were incubated with preimmune serum or anti-CPD/CPD-N antibodies followed by the secondary AlexaFluor 488 goat anti-rabbit IgG conjugate. Propidium iodide (PI) staining of the nucleus was performed as the last step. The morphological changes seen in K562 myeloma cells after exposure to IL-2 for 24 h are not unusual. Quiescent Nb2 lymphoma cells also have large cell nuclei surrounded by a little cytoplasm, but PRL treatment resulted in a robust cytoplasm in 24 h [12,38].

pH range. Indeed, Figure 10 confirms that CPD-N has a single optimum pH of 5.6, whereas CPD exhibits optimal activity at pH 5.6 and for pH 6.5–7.0.

DISCUSSION

Our studies showed that, like the prototypic 180 kDa rat CPD, the nuclear 160 kDa CPD-N is a catalytically active enzyme. Cytokine stimulation of CPD-N expression suggests a role for PRL and IL-2 in polypeptide processing in the nucleus of haematopoietic cells. We originally identified CPD-N as a PRL-inducible cDNA in the rat Nb2 lymphoma cell line with 99.9 % nucleotide identity with the rat CPD cDNA [12]. However, the 5′-end of the full-length CPD-N cDNA appeared to be truncated when compared with the CPD cDNA. The origin of the CPD-N transcript was not known. Analysis of the rat genome now suggests that the CPD gene is transcribed at an alternative start site downstream of exon 1 to produce the CPD-N transcript (Figure 1). Exon 1 of the CPD gene encodes the CP domain I but the downstream cryptic

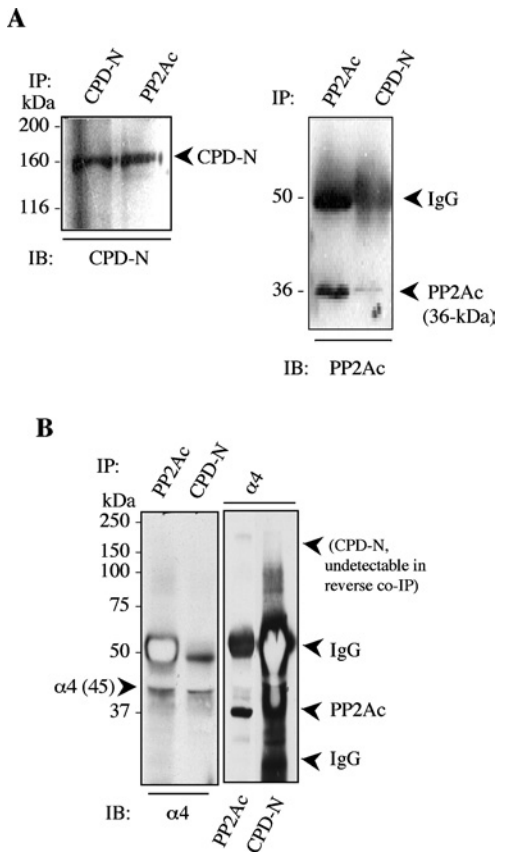

Figure 5 CPD-N interacts with PP2Ac and α4 phosphoprotein

(**A**, **B**) Nb2 cell homogenates were immunoprecipitated (IP) with anti-CPD-N, anti-PP2Ac or anti-α4 phosphoprotein antibodies as described in the Materials and methods section. Immunocomplexes were resolved by SDS/PAGE. Immunoblotting (IB) was performed with anti-CPD-N, anti-PP2Ac or anti-α4 antibodies as indicated. In (**B**), blots were overexposed for CPD-N (undetectable).

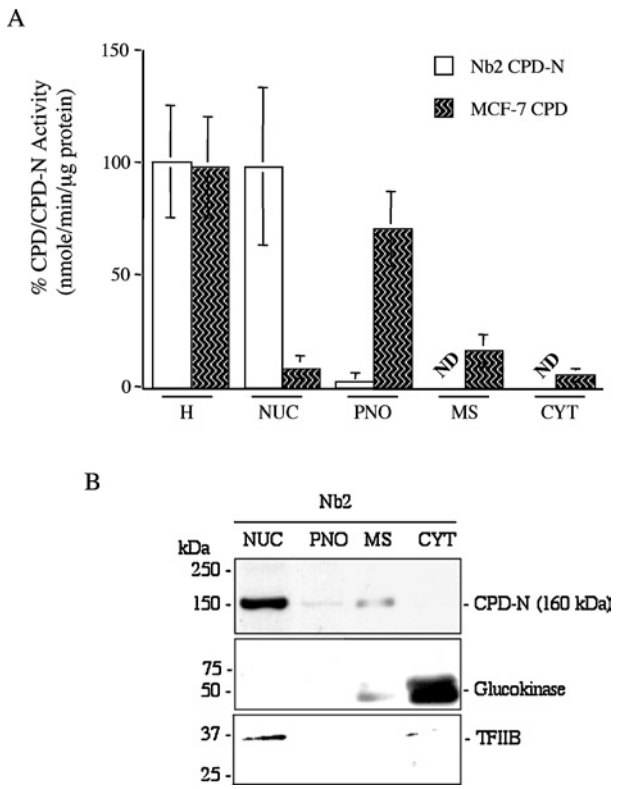

Figure 6 Distribution of CPD/CPD-N activity in Nb2 and MCF-7 cells

(**A**) Nb2 and MCF-7 fractions were used for CPD-N and CPD assays respectively. Enzyme activity was determined as the difference in activity measured in the presence or absence of the specific CPD inhibitor MGTA as described in the Materials and methods section. H, whole cell homogenate; NUC, nucleus, 700 ***g*** pellet; PNO, post-nuclear, 10000 ***g*** pellet; MS, microsomes, 100000 ***g*** pellet; CYT, cytosol, 100000 ***g*** supernatant. CPD-N (Nb2) activity was predominantly in the NUC fraction, whereas CPD (MCF-7) activity was mainly in the PNO and MS fractions. ND, not significant. Results shown are representative of three independent experiments (means $\pm$ S.D.; $n = 3$). (**B**) Western analysis of Nb2 cell fractions.

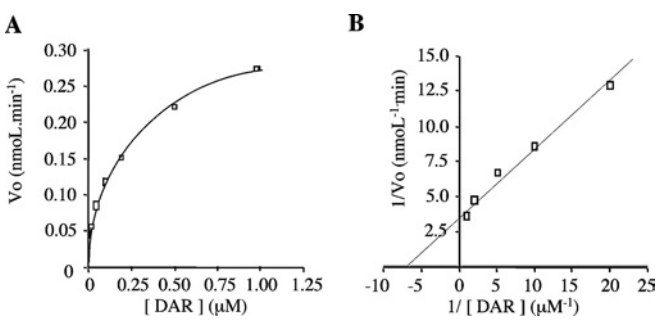

Figure 7 Kinetics of CPD-N activity

Nb2 nuclear fraction (20 μg of protein/assay) was used for CPD-N assay using dansyl-L-alanyl-L-arginine (DAR) as substrate. (**A**) Michaelis–Menten plot and (**B**) Lineweaver–Burk plot of Nb2 CPD-N. Results shown are representative of six independent experiments ($n = 6$). A similar kinetics analysis was performed for the MCF-7 CPD using the 10000 ***g*** pellet (15 μg of protein/assay) (see Table 1).

exon 1′, demarcated by classical intron–exon splice sequences (agGT-AGgt), encodes the N-terminus of CPD-N. A 160 kDa CPD-N-like protein appears to be frequently expressed in a number of haematopoietic tumour cells. An NCBI EST (expressed sequence tag) database search failed to identify the CPD-N cDNA sequence in normal mammalian tissues, suggesting that its expression may be restricted by cell lineage or tumour phenotype. Furthermore, unlike most vertebrate mRNAs, which use the Kozak consensus sequence (gcc)a/gccATGg for initiation of translation [24], translation of the Nb2 CPD-N mRNA is predicted to occur at cagATGa to yield the 160 kDa gene product (Figure 1). However, there are many examples of non-conventional Kozak sequences (http://www.changbioscience.com/primo/human.html), including usage of the same cagATGa sequence in translation initiation of human forkhead transcription factor FREAC2 (AF084938), forkhead FOXF2 (NM001452), IL-11 receptor α-chain (BC003110) and synapsin IIb (U40215).

Alternative exon usage has been reported for other CP-like enzymes. When the *Drosophila melanogaster* silver (*svr*) gene was first cloned, it was identified to encode multiple preprotein-processing carboxypeptidases similar to human CPE, CPM, and CPN [25]. The *Drosophila svr* gene has eight exons and actually encodes a 'long' form of a CPD-like protein that has three CP-like domains, followed by a transmembrane domain and a cytosolic tail [26]. The *svr* gene has three alternatively spliced first exons (exons 1A, 1B and 1C), and use of either exon 1A or 1B results in expression of 'long' CPD-like proteins with different N-terminal domains (either 1A or 1B). In addition, 'short' forms of the enzyme are produced that only have the first domain (1A or 1B) but not domain 2 or 3. The N-terminal regions of the proteins encoded by the first ATGs in exons 1A and 1B are predicted to encode signal peptides, whereas exon 1C encodes a protein that

Table 1 CPD/CPD-N kinetics with dansyl-L-alanyl-L-arginine as substrate

Results are means ± S.D. ($n = 6$) for MCF-7 CPD and Nb2 CPD-N.

Parameter	MCF-7 CPD	Nb2 CPD-N
V_{max} (μmol/min)	27.0 ± 1.0	269.0 ± 53.0
K_m (μM)	63.0 ± 9.0	132.0 ± 30.0
10^{-2} × SA (units/mg of protein)	0.180 ± 0.007	1.35 ± 0.27

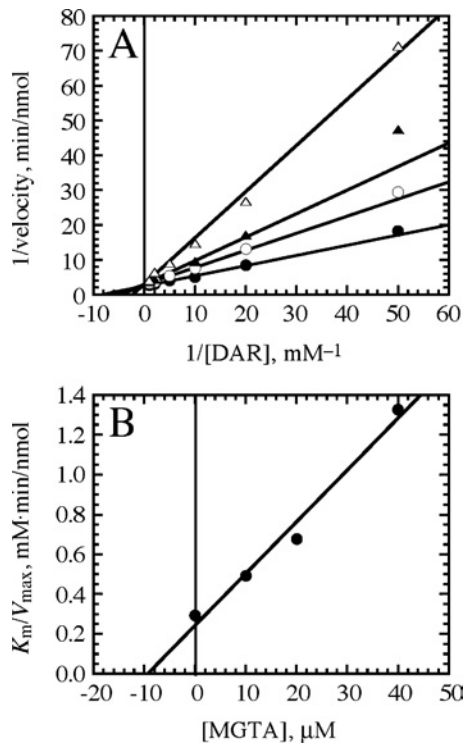

Figure 8 Inhibition of CPD-N by MGTA

(**A**) Double-reciprocal Lineweaver–Burk plot of CPD-N activity in Nb2 nuclear fractions in the presence of MGTA. (**B**) Reciprocal slopes, obtained from the initial velocity curves, were plotted as a function of MGTA concentrations. Results shown are representative of four independent experiments. Similar inhibition experiments ($n = 4$) were performed for the MCF-7 CPD (see Table 2).

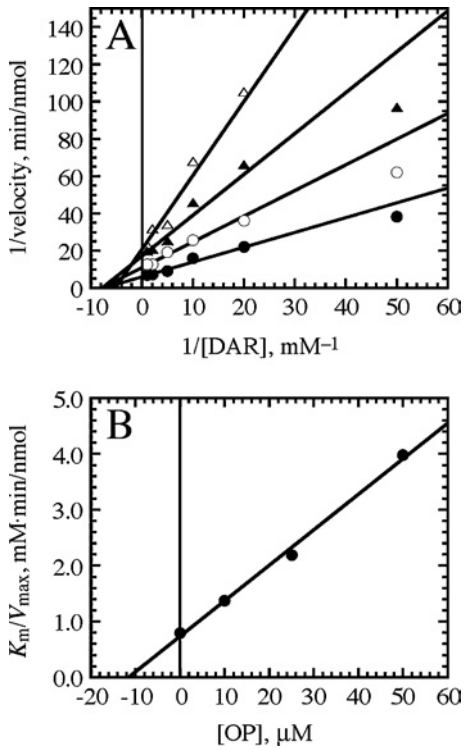

Figure 9 Inhibition of CPD-N by OP

(**A**) Double-reciprocal Lineweaver–Burk plot of CPD-N activity in Nb2 nuclear fractions in the presence of OP. (**B**) Reciprocal slopes, obtained from the initial velocity curves, were plotted as a function of OP concentrations. Results shown are representative of four independent experiments. A similar inhibition kinetic analysis ($n = 3$) was performed for the MCF-7 CPD (see Table 2).

Table 2 Inhibition of CPD and CPD-N by MGTA or OP

Results are means ± S.D. ($n = 3$) for CPD and CPD-N.

	K_i (μM)	
Inhibitor	MCF-7 CPD	Nb2 CPD-N
MGTA	47.6 ± 5.9	9.3 ± 2.5
OP	45.1 ± 6.8	11.6 ± 1.4

lacks a signal peptide but which has a truncated CP-like domain. When individual domains of the *Drosophila* CPD were expressed, domains 1B and 2, but not 1A, were found to be enzymatically active, cleaving substrates with a C-terminal arginine or lysine residue. Domain 1B was more active at neutral pH and greatly preferred C-terminal arginine to lysine, whereas domain 2 was more active at pH 5–6 and slightly preferred C-terminal lysine to arginine. These properties of the *Drosophila* domains 1B and 2 are similar to those of domains 1 and 2 of the CPD in duck [4] and mammals [8,13,27]. The conservation of these enzymatic properties (optimum pH and substrate specificity) of the first two domains has been suggested to be essential to CPD function [26]. On the other hand, the nuclear CPD-N is enzymatically active, indicating that CPD-like enzymes without an intact domain I are functional but, due to its domain II, has optimal activity at a pH of approx. 5.6.

The full-length CPD has three CP enzyme homology domains with amino acid residues from about 86–381 making up domain I. The N-terminal 249 residues in CPD are absent from CPD-N and their absence not only results in an inactive domain I but also in loss of the signal peptide in CPD-N. In the full-length CPD, the signal peptide and the C-terminal transmembrane domain are believed to interact co-operatively to form a hydrophobic transmembrane region that permits CPD to insert into the TGN membrane [9,19,23]. The absence of a signal peptide in the 160 kDa CPD-N may account for its diffuse distribution, not in the TGN, but within the nucleus of Nb2 cells [12] and K562 cells (Figure 4).

Novikova et al. [4] previously reported that domain I of CPD (optimum pH of 6.5–7.0) had a greater affinity for substrates with a C-terminal arginine residue, whereas domain II (optimum pH of 5.6) preferentially bound substrates with a C-terminal lysine residue. This substrate specificity is consistent with our observation that CPD-N, with only domain II, exhibited a reduced affinity (132 ± 30 μM) for dansyl-L-alanyl-L-arginine relative to CPD with its domain I (63 ± 9 μM). However, comparison

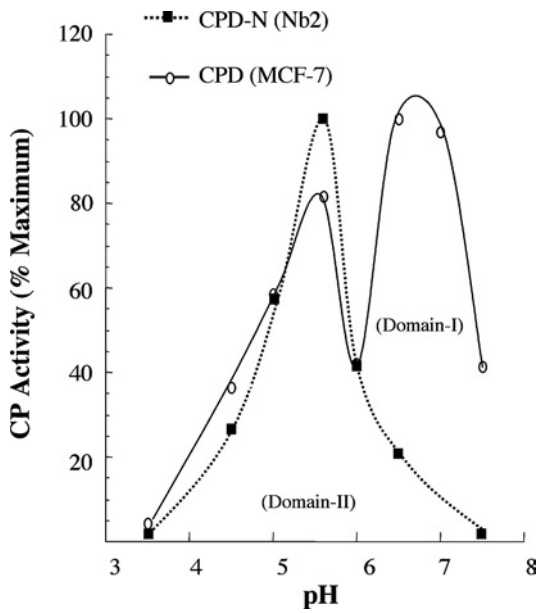

Figure 10 Effect of pH on CP activities

(**A**) Nb2 CPD-N. (**B**) MCF-7 CPD. Activity was normalized to the maximal activity detected at the optimal pH for each enzyme. Each plot is representative of three independent experiments.

of the specific activity/K_m ratios reveals that dansyl-L-alanyl-L-arginine is a better substrate for CPD-N than CPD. Our studies also confirmed that CPD (in MCF-7 cells) has two optimum pH values at 5.6 and 6.5–7.0, due to its domains II and I respectively, whereas CPD-N has only a single optimum pH at 5.6 due to domain II. The finding that CPD-N has an acidic optimum pH raises the question of whether it is active in the cell nucleus. Nuclear enzymes that display acidic optimum pH *in vitro* have been reported. These include a family of nucleases, exemplified by DNase II, that are implicated in apoptotic DNA digestion [28,29] and a recently characterized acidic nuclease/intra-cyclobutyl-pyrimidine-dimer-DNA phosphodiesterase that may function in apoptotic DNA digestion as well as in metabolism of cyclobutyl pyrimidine primers in UV-irradiated cells [30]. The broad pH range of CPD is believed to facilitate the processing of polypeptides transiting the length of the secretory pathway within the TGN and immature vesicles [4,6–8]. Although the physiological substrate(s) of CPD-N is not yet known, its pH–activity profile suggests that its potential substrate(s) may contain C-terminal arginine residues.

CPD is known to undergo post-translational modification, including palmitoylation and phosphorylation [10,20,31]. The cytoplasmic tail of CPD can be phosphorylated by purified protein kinase A, protein kinase C and CK2 [20]. The CPD tail also interacts with PP2A [20]. The binding of the CPD tail does not influence the catalytic activity of PP2A, but PP2A is involved in the trafficking of CPD from the TGN to the plasma membrane [20]. The α4 phosphoprotein is a known protein partner of PP2Ac [14,21] and is implicated as a positive regulator of PP2A activity [32]. The nuclear substrates for CPD-N are not known, but our demonstration of a CPD-N–α4–PP2Ac complex implicates a potential role for α4–PP2Ac in CPD-N action.

The hCPD gene and its promoter (a total of $\sim$88.3 kb) were recently characterized [33]. The hCPD gene contains 21 introns and has multiple transcription start sites. The promoter region of the hCPD gene lacks a TATA box but contains three GC boxes and the binding site for the transcription factor Sp1 and a putative site for nuclear factor κB. Timblin et al. [33] pointed out that Sp1 is essential for regulating the expression of several myeloid-specific genes, for example, through Sp1 binding to the promoters of CD11B [34] and the proto-oncogene c-*fes* [35]. Sp1 is also associated with PRL-responsive genes in lymphoid tumour cells [36,37]. Since the rat CPD-N and CPD transcripts are derived from the same CPD gene, Sp1 probably plays a role in the PRL-inducible expression of both these transcripts. In future studies, the potential interaction between Sp1 and the CPD/CPD-N gene promoter will be examined by chromatin immunoprecipitation assays.

In summary, we have demonstrated that cytokine-inducible CPD-N is expressed in several haematopoietic tumour cell lines. Specific protein–protein interaction at the C-terminal end of CPD, such as with PP2Ac, is preserved in CPD-N. In addition, we have demonstrated that CPD-N is a catalytically active metallocarboxypeptidase that acts optimally at pH 5.6 due to its intact domain II. In contrast, CPD, with intact domains I and II, acts over a much broader pH range.

We are grateful to Dr M. Baguma-Nibasheka (Department of Physiology and Biophysics, Dalhousie University) for providing slides of unstained K562 cells. We thank Dr N. Ridgway (Department of Biochemistry and Molecular Biology, Dalhousie University) and Dr P. Murphy (Department of Physiology and Biophysics, Dalhousie University) for their critical reading of this paper and helpful suggestions. This work was funded by the Canadian Institutes of Health Research (MOP12895; to C. K. L. T.) and the Breast Cancer Foundation Atlantic Chapter (to C. K. L. T. and S. L. B.).

REFERENCES

1 Skidgel, R. A. and Erdos, E. G. (1998) Cellular carboxypeptidases. Immunol. Rev. **161**, 129–141
2 Kuroki, K., Eng, F., Ishikawa, T., Turck, C., Harada, F. and Ganem, D. (1995) gp180, a host cell glycoprotein that binds duck hepatitis B virus particles, is encoded by a member of the carboxypeptidase gene family. J. Biol. Chem. **270**, 15022–15028
3 Eng, F. J., Novikova, E. G., Kuroki, K., Ganem, D. and Fricker, L. D. (1998) gp180, a protein that binds duck hepatitis B virus particles, has metallocarboxypeptidase D-like enzymatic activity. J. Biol. Chem. **273**, 8382–8388
4 Novikova, E. G., Eng, F. J., Yan, L., Qian, Y. and Fricker, L. D. (1999) Characterization of the enzymatic properties of the first and second domains of metallocarboxypeptidase D. J. Biol. Chem. **274**, 28887–28892
5 Aloy, P., Companys, V., Vendrell, J., Aviles, F. X., Fricker, L. D., Coll, M. and Gomis-Ruth, F. X. (2001) The crystal structure of the inhibitor-complexed carboxypeptidase D domain II and the modeling of regulatory carboxypeptidases. J. Biol. Chem. **276**, 16177–16184
6 Song, L. and Fricker, L. D. (1995) Purification and characterization of carboxypeptidase D, a novel carboxypeptidase E-like enzyme, from bovine pituitary. J. Biol. Chem. **270**, 25007–25013
7 Song, L. and Fricker, L. D. (1996) Tissue distribution and characterization of soluble and membrane-bound forms of metallocarboxypeptidase D. J. Biol. Chem. **271**, 28884–28889
8 Tan, F., Rehli, M., Krause, S. W. and Skidgel, R. A. (1997) Sequence of human carboxypeptidase D reveals it to be a member of the regulatory carboxypeptidase family with three tandem active site domains. Biochem. J. **327**, 81–87
9 Varlamov, O., Eng, F. J., Novikova, E. G. and Fricker, L. D. (1999) Localization of metallocarboxypeptidase D in AtT-20 cells. Potential role in prohormone processing. J. Biol. Chem. **274**, 14759–14767
10 Kalinina, E., Varlamov, O. and Fricker, L. D. (2002) Analysis of the carboxypeptidase D cytoplasmic domain: implications in intracellular trafficking. J. Cell. Biochem. **85**, 101–111
11 Hadkar, V. and Skidgel, R. A. (2001) Carboxypeptidase D is up-regulated in RAW 264.7 macrophages and stimulates nitric oxide synthesis by cells in arginine-free medium. Mol. Pharmacol. **59**, 1324–1332
12 Too, C. K. L., Vickaryous, N., Boudreau, R. T. and Sangster, S. M. (2001) Identification and nuclear localization of a novel prolactin and cytokine-responsive carboxypeptidase D. Endocrinology **142**, 1357–1367
13 Xin, X., Varlamov, O., Day, R., Dong, W., Bridgett, M. M., Leiter, E. H. and Fricker, L. D. (1997) Cloning and sequence analysis of cDNA encoding rat carboxypeptidase D. DNA Cell Biol. **16**, 897–909

14 Boudreau, R. T. M., Sangster, S. M., Johnson, L. M., Dauphinee, S., Li, A. W. and Too, C. K. L. (2002) Implication of α4 phosphoprotein and the rapamycin-sensitive mTOR pathway in prolactin receptor signalling. J. Endocrinol. **173**, 493–506

15 Too, C. K. L., Cragoe, Jr, E. J. and Friesen, H. G. (1987) Amiloride-sensitive Na^+/H^+ exchange in rat Nb2 node lymphoma cells. Stimulation by prolactin and other mitogens. Endocrinology **121**, 1512–1520

16 Fricker, L. D. and Snyder, S. H. (1982) Enkephalin convertase: purification and characterization of a specific enkephalin-synthesizing carboxypeptidase localized to adrenal chromaffin granules. Proc. Natl. Acad. Sci. U.S.A. **79**, 3886–3890

17 Fricker, L. D., Supattapone, S. and Snyder, S. H. (1982) Enkephalin convertase: a specific enkephalin synthesizing carboxypeptidase in adrenal chromaffin granules, brain, and pituitary gland. Life Sci. **31**, 1841–1844

18 Tan, F., Deddish, P. A. and Skidgel, R. A. (1995) Human carboxypeptidase M. Methods Enzymol. **248**, 663–675

19 Varlamov, O. and Fricker, L. D. (1998) Intracellular trafficking of metallocarboxypeptidase D in AtT-20 cells: localization to the trans-Golgi network and recycling from the cell surface. J. Cell Sci. **111**, 877–885

20 Varlamov, O., Kalinina, E., Che, F. Y. and Fricker, L. D. (2001) Protein phosphatase 2A binds to the cytoplasmic tail of carboxypeptidase D and regulates post-trans-Golgi network trafficking. J. Cell Sci. **114**, 311–322

21 Chen, J., Peterson, R. T. and Schreiber, S. L. (1998) Alpha 4 associates with protein phosphatases 2A, 4, and 6. Biochem. Biophys. Res. Commun. **247**, 827–832

22 Inui, S., Sanjo, H., Maeda, K., Yamamoto, H., Miyamoto, E. and Sakaguchi, N. (1998) Ig receptor binding protein 1 (alpha4) is associated with a rapamycin-sensitive signal transduction in lymphocytes through direct binding to the catalytic subunit of protein phosphatase 2A. Blood **92**, 539–546

23 Varlamov, O., Wu, F., Shields, D. and Fricker, L. D. (1999) Biosynthesis and packaging of carboxypeptidase D into nascent secretory vesicles in pituitary cell lines. J. Biol. Chem. **274**, 14040–14045

24 Kozak, M. (1987) An analysis of 5′-noncoding sequences from 699 vertebrate messenger RNAs. Nucleic Acids Res. **15**, 8125–8148

25 Settle, Jr, S. H., Green, M. M. and Burtis, K. C. (1995) The silver gene of Drosophila melanogaster encodes multiple carboxypeptidases similar to mammalian prohormone-processing enzymes. Proc. Natl. Acad. Sci. U.S.A. **92**, 9470–9474

26 Sidyelyeva, G. and Fricker, L. D. (2002) Characterization of Drosophila carboxypeptidase D. J. Biol. Chem. **277**, 49613–49620

27 Ishikawa, T., Murakami, K., Kido, Y., Ohnishi, S., Yazaki, Y., Harada, F. and Kuroki, K. (1998) Cloning, functional expression, and chromosomal localization of the human and mouse gp180-carboxypeptidase D-like enzyme. Gene **215**, 361–370

28 Walker, P. R. and Sikorska, M. (1997) New aspects of the mechanism of DNA fragmentation in apoptosis. Biochem. Cell Biol. **75**, 287–299

29 Thompson, E. B. (1998) Special topic: apoptosis. Annu. Rev. Physiol. **60**, 525–532

30 Famulski, K. S., Liuzzi, M., Bashir, S., Mirzayans, R. and Paterson, M. C. (2000) Purification and characterization of a novel human acidic nuclease/intra-cyclobutyl-pyrimidine-dimer-DNA phosphodiesterase. Biochem. J. **345**, 583–593

31 Eng, F. J., Varlamov, O. and Fricker, L. D. (1999) Sequences within the cytoplasmic domain of gp180/carboxypeptidase D mediate localization to the trans-Golgi network. Mol. Biol. Cell **10**, 35–46

32 Short, K. M., Hopwood, B., Yi, Z. and Cox, T. C. (2002) MID1 and MID2 homo- and heterodimerise to tether the rapamycin-sensitive PP2A regulatory subunit, alpha 4, to microtubules: implications for the clinical variability of X-linked Opitz GBBB syndrome and other developmental disorders. BMC Cell Biol. **3**, 1

33 Timblin, B., Rehli, M. and Skidgel, R. A. (2002) Structural characterization of the human carboxypeptidase D gene and its promoter. Int. Immunopharmacol. **2**, 1907–1917

34 Chen, H.-M., Pahl, H. L., Scheibe, R. J., Zhang, D.-E. and Tenen, D. G. (1993) The Sp1 transcription factor binds the CD11b promoter specifically in myeloid cells *in vivo* and is essential for myeloid-specific promoter activity. J. Biol. Chem. **268**, 8230–8239

35 Heydemann, A., Juang, G., Hennessy, K., Parmacek, M. S. and Simon, M. C. (1996) The myeloid-cell-specific c-fes promoter is regulated by Sp1, PU.1, and a novel transcription factor. Mol. Cell. Biol. **16**, 1676–1686

36 Too, C. K. L. (1997) Induction of Sp1 activity by prolactin and interleukin-2 in Nb2 T cells: differential association of Sp1-DNA complexes with Stats. Mol. Cell. Endocrinol. **129**, 7–16

37 Book McAlexander, M. and Yu-Lee, L. Y. (2001) Sp1 is required for prolactin activation of the interferon regulatory factor-1 gene. Mol. Cell. Endocrinol. **184**, 135–141

38 Johnson, L. M. and Too, C. K. L. (2001) Prolactin, interleukin-2 and FGF-2 stimulate expression, nuclear distribution and DNA-binding of rat homolog of pombe Cdc5 in Nb2 T lymphoma cells. Mol. Cell. Endocrinol. **184**, 151–161

Received 4 January 2005/20 May 2005; accepted 27 May 2005
Published as BJ Immediate Publication 27 May 2005, doi:10.1042/BJ20050025